Static and Dynamic Performance Evaluation of a 3-DOF Spindle Head using CAD-CAE Integration Methodology

Yue Ma [a], Wentie Niu [a,*], Zhenjun Luo [a], Fuwen Yin [a], Tian Huang [a,b]

[a] *Key Laboratory of Mechanism Theory and Equipment Design of The State Education Ministry, Tianjin University, Tianjin 300072, China*
[b] *School of Engineering, The University of Warwick, Coventry CV4 7AL, UK*
** Corresponding Author. Tel: +86 13011303319; fax: +86 022 27406260; E-mail address: niuwentie@gmail.com*

Abstract: Accurate and rapid modeling and performance evaluation over the entire workspace is a crucially important issue in the design optimization of parallel kinematic machines (PKMs), especially for those dedicated for high-speed machining where high rigidity and high dynamics are the essential requirements. By taking a 3-DOF spindle head named A3 head as an example, this paper presents a feature-based CAD-CAE integration methodology for the static and dynamic analyses of PKMs. The approach can be implemented by four steps: (1) creation of a parameterized geometric (CAD) model with analysis features in SolidWorks; (2) extraction of the features from the CAD model using the Application Programming Interface (API) available in SolidWorks; (3) formulation of a CAD model in SAMCEF by mapping the configuration features from SolidWorks to SAMCEF; and (4) conversion of the analysis features into a scripting language named Bacon for Finite Element Analysis (FEA). The merit of this approach lies in that the FE model at different configurations can be updated automatically in batch mode, and PKM having different topologies can be modeled with ease thanks to the down to link/joint level featuring. The experiment is also carried out to verify the effectiveness of the proposed approach.

Keywords: Parallel kinematic machines, CAD-CAE Integration, Performance evaluation, Finite Element Analysis

1. Introduction

Static and dynamic compliances are the significant performance indices of parallel kinematic machines (PKMs) [1-2] especially for those dedicated to implementing high-speed machining and forced assembly, etc., where high rigidity and high dynamics are crucially required. In order to avoid time and cost-intensive manufacturing and testing of physical prototypes, it is preferable to employ "virtual prototyping" technology [3-5] such that a computer simulation model can be built, analyzed and tested like a real machine in a time and cost effective manner. Considering the complex 3D geometries of the components, the virtual machine of a PKM should be built with the aid of commercial CAD and CAE software. Meanwhile, it is expected that the models can be rapidly reconfigured within a family having similar joints/links at the component level, and for each model, the static and dynamic performances over the task workspace can be evaluated in a quick manner.

Literature reveals intensive investigations in the past decades towards bridging the gaps between CAD and CAE tools. The approaches available to hand can roughly be classified into three categories, i.e., the CAE-centric integration, the CAD-centric integration and the feature-based integration. In the CAE-centric integration [6-7], both geometric (CAD) and FE (finite element) models are built and parameterized under the CAE environment so that they can be updated automatically at different configurations by Parametric Design Languages (PDL) embed in the system, APDL (ANSYS Parametric Design Language) for ANSYS, PCL (Patran Command Language) for MSC/Patran and Bacon (a script language that can be used to mimic GUI operations) for SAMCEF for example. However, the limited capability of CAD builder embed in such a system makes it difficult to deal with geometric modeling of components having complex geometry. In order to solve this problem, the CAD-centric integration [8-12] is developed by implementing three successive steps, i.e., geometric modeling in a CAD tool, geometric data transfer from the CAD tool to a CAE tool *via* the third-party interfaces, e.g., STEP, IGES and STL, and FE analysis by means of corresponding PDL programming. However, the models for different machines have to be built in a one-by-one manner even if they have same or at least similar joints/links at the component level. To overcome the limitations mentioned above, the feature-based technology [13-18] has been intensively investigated in the past decades thanks to its capability to capture geometric and non-geometric information of the modularized components in an object-oriented manner. Along this track, a plenty of efforts have been made to develop the feature-based CAD-CAE integration systems. For instance, Arabshahi *et al* seems to be the first to develop such a system that allows CAD-FEA data to be exchanged automatically using the tools that can operate directly on the solid model [19]. As there is no generic, unified model to allow both design and analysis information to be specified, Deng *et al* proposed a feature-based CAD-CAE integration system for injection-mold design by creating an input file containing all the information required for FEA [20]. By studying the mapping relationship between analysis features and APDL, Niu *et al* developed a feature-based integration system that can be readily used for FE modeling and analysis of machine tools [21]. In order to realize the bidirectional integration of CAD and CAE, Lee proposed a CAD-CAE integration system by multi-resolution feature modeling techniques in a unified and synchronous modeling environment [22]. The system created and manipulated a single master model containing all information required for CAD and CAE such that the design and analysis can be carried out in an interactive manner.

More recently, several attempts have been made to deal with the CAD-CAE integration using a unified CAD and CAE model. Gujarathi *et al* developed a promising CAD-CAE parametric integration method using a neutral data model called Common Data

Model (CDM) [23]. The merit of this model lies in that the design and analysis can be integrated via the associative relations and the built-in interfaces of CAD and CAE models, and it thereby provides better flexibility for the use of various commercial CAD and CAE software. Hamri *et al* proposed a software environment for CAD-CAE integration based on the mixed shape representations maintained on the same topology support called the High Level Topology (HLT) [24]. The system improves the robustness of various processes involved in FE model preparation from CAD data and made the conversion more efficient. Xia *et al* presented an incorporate CAD-CAE software framework using the Unified Representation Architecture (URA) and a geometric modeling engine-ACIS, allowing an incorporate CAD-CAE operation in the same software interface [25]. Since all pieces of the design and analysis information can be treated as design feature by URA, the loop of design-analysis-redesign can be performed in an automatic manner. In order to integrate CAD-CAE integration and CAE modeling continuously, Kong *et al* presented a rapid integrated parametric CAE modeling method based on a script template in Linear Variable Differential Transformer (LVDT) simulations [26]. Examples show that the parametric LVDT simulation can not only be rapidly established but also effectively used to improve the quality of LVDT design. By developing a new Heterogeneous Feature Model (HFM) for model transferring, Liu *et al* proposed a novel CACD-CAD-CAE integrated framework for design, modeling and optimization of fiber-reinforced plastic parts [27]. As all modules in this system share a common HFM, design automation can be realized in certain stages of the design process, and the dependency on manual decisions can be evidently reduced.

Driven by many practical needs in PKM design, this paper presents a feature-based CAD-CAE integration system to evaluate the static and dynamic performances of a 3-DOF spindle head named A3 head especially designed for high-speed machining [28-29]. Having addressed the significance and the existing problems to be tackled in virtual prototyping of PKMs, the rest of this paper is organized as follows. After a brief introduction to the mechanical design of the A3 head in Section 2, a framework and the detailed procedures of the feature-based CAD-CAE integration approach are proposed in Section 3 using the powerful geometric modeling capability of SolidWorks™ (2010) and FEA capability of SAMCEF™ (V8.2). Then, the proposed approach is employed to evaluate the static and dynamic performances of the A3 head over the task workspace with the verification by the experiments in Section 4 before the conclusions are drawn in Section 5.

2. System description [29]

Fig.1 shows a CAD model of the A3 head, the architecture behind is a 3-RPS parallel mechanism that consists of a moving platform, a base and three identical RPS limbs. Here, R and S represent a revolute and a spherical joint, respectively, and the underlined P denotes an active prismatic joint. Independently driven by the three servomotor lead-screw assemblies, the platform achieves three degrees of freedom in terms of one translation and two rotations. An electrical spindle can be mounted on the platform to implement high-speed milling. The design features of the A3 head are, in brief: The revolute joint connecting the limbs to the base is elaborately designed around an oblong-shaped closed frame in order to achieve a compact, lightweight yet rigid mechanical design. Two opposing short half-shafts project from the frame, rigidly fixed to the inner rings of bearings that have outer rings mounted within block units attached to the base. Internally, each side of the closed frame carries one element of a ball guideway, the other elements are mounted on each side of the limb body. The closed frame also carries the nut of the lead-screw assembly. The limb body carries a servo-motor and lead-screw thrust-bearing to the rear and a spherical bearing to the front. The limb body is designed as a hollow rectangular structure having inner stiffeners, dished on one side to accommodate the lead-screw. Its cross-section dimensions are set to keep overall sizes and weight as low as practicable, while providing adequate bending rigidity against deflections caused by the constraint forces imposed at center of the spherical joint along the direction of the axis of the revolute joint. The block units facilitate assembly, being secured to the base by bolts and pins accessible from the rear. As a result, a compact, lightweight and rigid mechanical design is achieved.

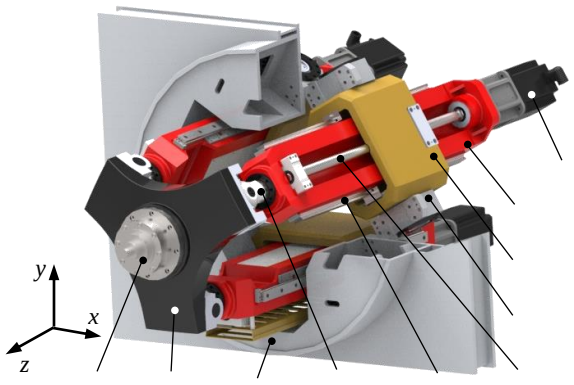

Similar to very successful applications of PKMs, e.g., the Tricept [30], the Exechon [31] and the Sprint Z3 head [32], the A3 head can also be used as a plug-and-play module to form a manufacturing system for large structural component machining.

3. Feature-Based CAD-CAE integration

By taking the A3 head as an example, a feature-based CAD-CAE integration approach for the static and dynamic analyses of PKMs is presented in this section with the emphases upon: (1) finite element modeling of commonly used joints, (2) development of a framework for the feature-based CAD-CAE integration, and (3) the feature modeling and mapping techniques from SolidWorks to SAMCEF.

3.1. Finite element modeling of joints

Finite element modeling of joints is a fundamental and essential step in either manual or automated static and dynamic analyses

of PKMs. In order to ensure the computational efficiency without losing accuracy, the finite element models of the commonly used joints can be formulated by the assembly elements provided by SAMCEF [33-34], and their stiffness and damping coefficients can be specified using the data given by product catalogues, handbooks and experimental measurements for ensuring the simulation fidelity.

Without losing generality, the finite element model of a 1-DOF joint can be built in SAMCEF by the process shown in Fig.2:

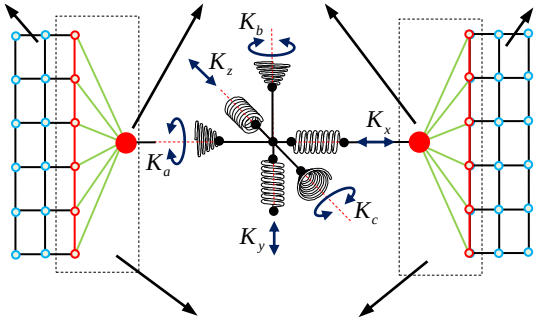

(1) On each meshed solid model of two adjacent components connected by a 1-DOF joint, select a group of nodes containing the contact region in terms of lines or faces.

(2) Establish a reference frame with its origin being the geometric center of the contact region and one coordinate axis being coincident with the joint axis. Let the node located at the origin be referred to as the virtual node. The virtual node may have already been included in the group of realistic nodes abovementioned. Otherwise, it should be created. This virtual node together with the group of realistic nodes constitutes a mean element. Assign the virtual node six degrees of freedom in terms of translation and rotation along/about three orthogonal axes. Then, the rigid body motions of all nodes within the mean element can be described by those of the virtual node.

(3) A 6-DOF bushing element as shown in Fig.2 can be used to connect two virtual nodes belonging to two mean elements to simulate the relative translational and rotational stiffness and damping of the joint along/about three orthogonal axes of the frame. Note that the stiffness and damping along/about the joint axis should be set to be zero for a passive joint, otherwise the actuated stiffness and damping should be considered.

The mean element here can be interpreted as a linear interpolation function to find the mean displacement and rotation of a set of concerned nodes, while the bushing element enables the stiffness and damping coefficients of the joint to be specified. These assembly elements can be combined in different ways to model multi-DOF joints according to their types and arrangements. For example, the spherical joint used in the A3 head can be modeled by the combination of three revolute joint having the joint axes orthogonal to one another. Fig.3 shows finite element models of joints and sub-assemblies used in a RPS limb of the A3 head built by the process.

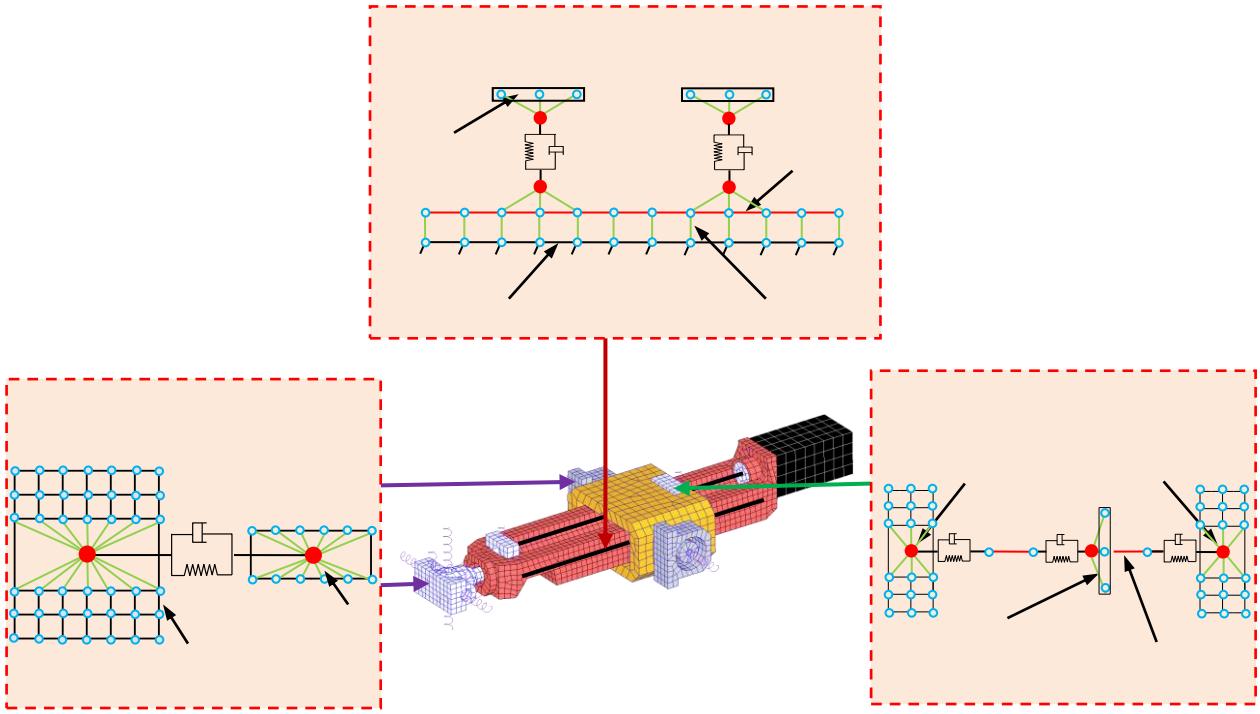

Fig.3. Joint FE models in the A3 head

3.2. Framework of the CAD-CAE integration system

As clearly indicated in Section 1, it is expected that the FE model of a PKM at different configurations can be automatically updated and rapidly reconfigured within a family having similar joints/links at the component level. To meet these requirements, a feature-based CAD-CAE integration approach is developed by exploiting the programming functionalities of SolidWorks and

SAMCEF. The term “feature” here indicates an informative unit representing a region of interest in a model and can be described by an aggregation of properties of the model. The relevant properties are referred to as feature attributes, including parametric values and their relations. A feature can be divided into several sub-features according to engineering semantic information necessary for design and analysis purposes. In the proposed feature-based CAD-CAE integration system, two sets of features, i.e., configuration features and analysis features are defined. The configuration (position and orientation) features contain a set of the configuration parameters of the local body-fixed frame in which the solid model of each component is built with respect to the reference frame of the machine as a whole because they cannot be captured by STEP/IGES. The analysis features include the element types and material properties associated with all components, the boundary conditions between the adjacent components connected by springs and dampers, and the payload imposed upon the output link. These features can be automatically extracted from the CAD model in SolidWorks using the Application Programming Interface (API) [35]. Combined with the solid models of components transferred to SAMCEF by STEP/IGES, these features can be used to generate the FE model of the system using the Notebook (an input file which can be used to define a set of variables) and Bacon (a script language that can be used to mimic GUI operations). Fig.4 shows the framework of the proposed feature-based CAD-CAE integration system with the modeling process that can be carried out by six steps as follows:

(1) Build a parameterized geometric (CAD) model having analysis features which are treated as attributes of the related geometric entities by interactive GUI operations in SolidWorks;

(2) Export the solid models at component level by STEP or IGES to SAMCEF;

(3) Extract the configuration features at component level using (1) and map them to SAMCEF;

(4) Build the geometric (CAD) model at the initial (home) configuration in SAMCEF based on (2) and (3);

(5) Extract the analysis features and convert them into the Bacon language format;

(6) Build the FE model in SAMCEF based on (4) and (5).

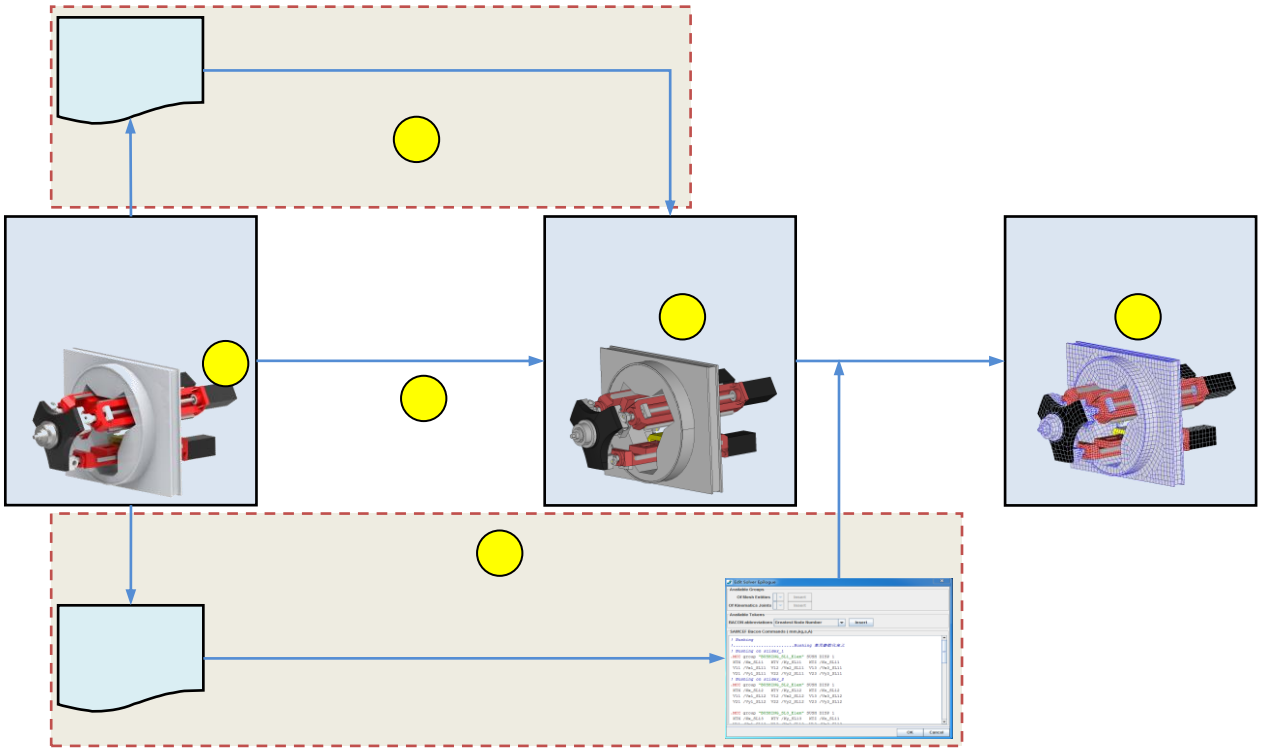

Fig.4. The flow chart of the proposed CAD-CAE integration

In this way, once the CAD model in SolidWorks is driven by the inverse kinematics to a specified configuration, its corresponding FE model can be modified automatically by mapping the updated features from SolidWorks to SAMCEF in a batch mode, and thus the static and dynamic performances at the corresponding configuration can be evaluated using the FE solver situated in SAMCEF. It is worthwhile pointing out that the proposed framework can accommodate other CAD software having API capabilities and other CAE tools having script languages similar to Bacon.

3.3. Feature modeling, mapping and updating

In this section, three key procedures, i.e., the analysis feature modeling, the configuration and analysis feature mappings for FE modeling of a PKM over the entire task workspace will be addressed in detail as follows.

3.3.1. Analysis feature modeling

It can be seen from Fig.4 that the first step in the proposed CAD-CAE integration system is to build a parameterized CAD model having analysis features in SolidWorks. Note that the analysis features must be attached to the related geometric entities built in SolidWorks in terms of points, lines, and faces. Hence, it is essential to define the analysis features that can be carried by the corresponding geometric entities which can be extracted from the CAD model built in SolidWorks.

With the aid of the object-oriented method, the analysis features are classified, at the component level, into two fundamental groups as shown in Fig.5, i.e., analysis features of a component and the analysis features between two connected components. The former can further be divided into a number of sub-features such as material feature, element feature, payload feature, etc. of the component itself. The latter contains the information necessary to describe the topological structure and parameters of the constraints provided by the mechanical joints. Note that the attributes assigned to each feature should be defined on the related geometric entities such that they can be extracted by SolidWorks API. Here, the attributes of material feature of a component include Young's modulus, mass density and Poisson ratio, etc. of the material used. The attributes of element feature indicate the element type defined on the related geometric entities of the component. The attributes of connection feature are related to the types, directions and parameters of constraints imposed between two connected components, the coordinates of the joint frame in which the stiffness and damping coefficients are defined for example. In addition, in order to reconfigure the PKMs at component/joint level in a quick manner, it would be more effective to generate the analysis features of a sub-assembly, a spherical joint for instance, by packaging a number of the fundamental analysis features of components and connections into a compound one using adequate data structure.

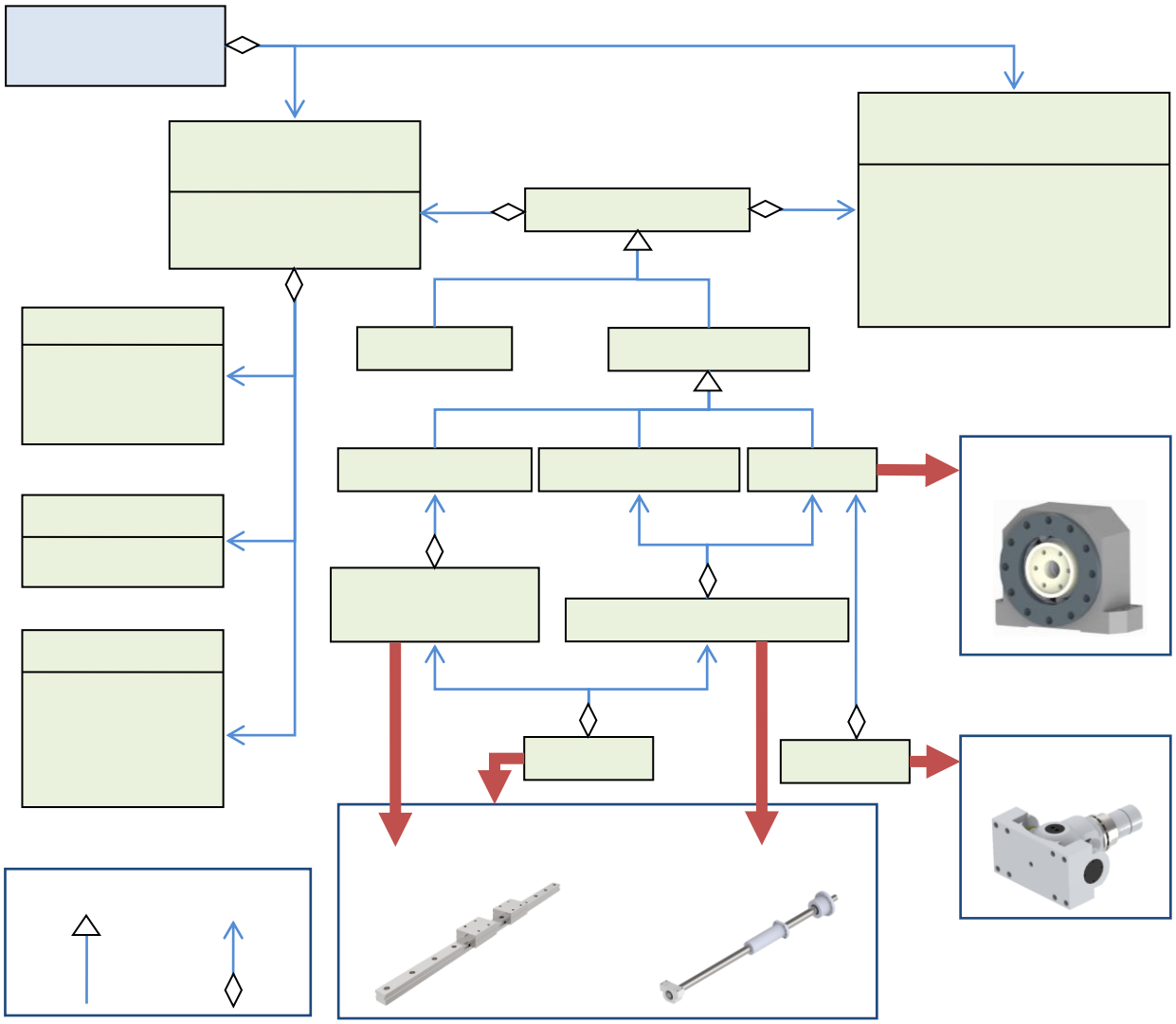

Fig.5. The object-oriented model of analysis features

Building upon the object-oriented model of analysis features, all the analysis features can be added to the corresponding geometric entities as SolidWorks attributes, and they can of course be modified if necessary. The process of the feature based modeling can be implemented as follows: (1) Select the type of analysis feature to be added; (2) Select the related geometric entities; (3) Assign the attributes of the selected analysis feature; (4) Attach the analysis feature as attributes to the selected

geometric entities using a prescribed data structure that can be extracted by SolidWorks API.

3.3.2. Configuration feature updating

As shown in Section 3.2, an important step in the proposed CAD-CAE integration system is to transport the configuration features at component level from SoildWorks to SAMCEF such that the corresponding solid models in SAMCEF can be uptated accordingly at a specific configuration. The configuration features of a component are defined as six parameters to describe the position and orientation of the local body-fixed frame in which the solid model of the component is built with respect to the reference frame of the machine as a whole. The configuration feature mapping can be done by two groups of processes.

(1) Building the CAD model in SAMCEF at the initial (home) configuration.

- Build the CAD model in SolidWorks at the initial (home) configuration;
- Export the corresponding solid models at component level to SAMCEF by IGES or STEP;
- Extract the configuration features at component level by API from the CAD model in SolidWorks. This operation can be programmed by Visual Basic.NET (VB.NET) with the SolidWorks API function called “Component2::Transform2”;
- Load the data file of configuration features by the Notebook in SAMCEF;
- Drive the solid models at component level in SAMCEF by the variables in the Notebook to build the CAD model in SAMCEF at the initial configuration.

(2) Updating the CAD model in SAMCEF at any specific configuration, as shown in Fig.6.

- For a specific configuration of the moving platform, determine the actuated joint variables, i.e., the limb lengths *via* the inverse displacement analysis [29]. This operation can be jointly programmed by VB.NET and MATLAB, and implemented by two steps, i.e., packaging the program of inverse displacement analysis in MATLAB as a standard Component Object Model (COM) using the Builder NE capability of MATLAB, and invoking this component in VB.NET to obtain the actuated joint variables;
- Drive the CAD model built in SolidWorks by the actuated joint variables to the specified configuration. This operation can be programmed by VB.NET and implemented by two steps, i.e., extracting the assembly information of the actuated joints using SolidWorks API, and modifying the assembly constraints using the API function called “Addmate3”;
- Extract the configuration features at component level by API from the CAD model in SolidWorks;
- Modify the CAD model in SAMCEF by the updated configuration features in the Notebook.

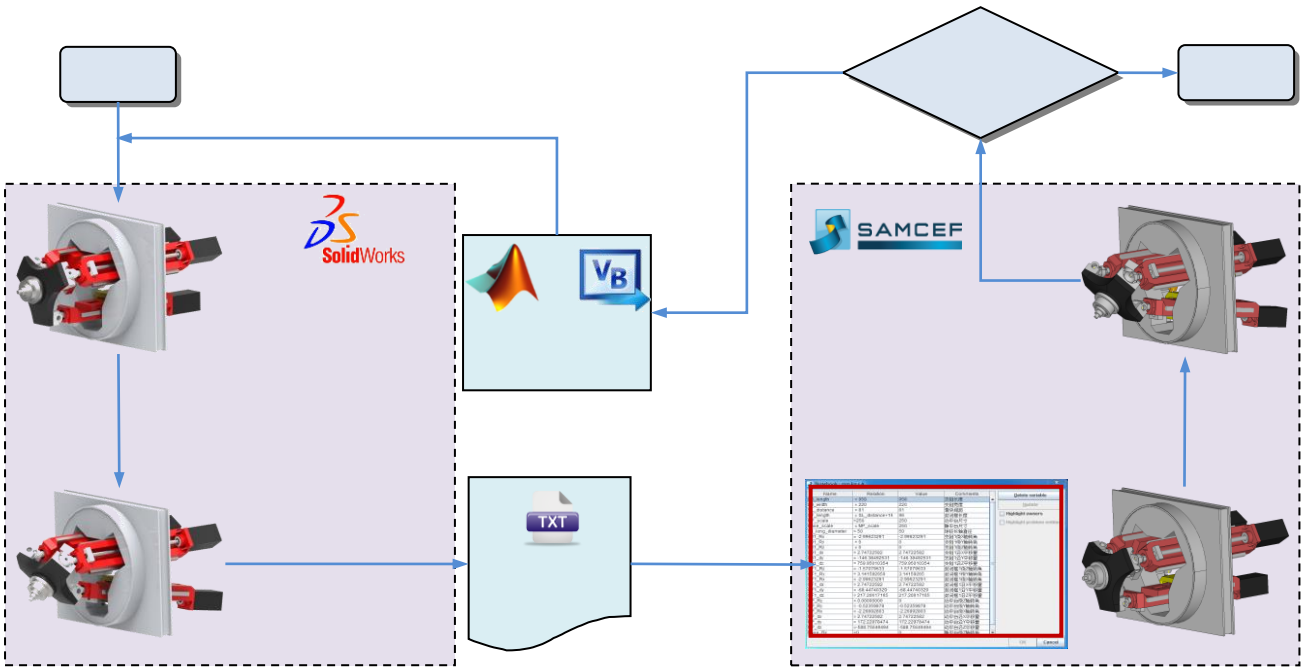

Fig.6. The process to update the configuration of the CAD model in SAMCEF

It can be seen that the merit of the process lies in that once the solid models at the initial configuration are transferred by STEP or IGES from SolidWorks to SAMCEF, the CAD model at any configuration in SAMCEF can be automatically modified by only updating the corresponding configuration features.

3.3.3. Analysis feature mapping

Referring to the flow chart of the CAD-CAE integration system shown in Fig.4, the FE model of a PKM at a given configuration can be generated automatically using the geometric models and the analysis features transported from SolidWorks to SAMCEF at the component level. Here, the attributes of analysis features are required to be assigned to the keywords (see

Table 1) defined as the Bacon commands. In order to ensure the efficiency of this assignment, two types of elementary command templates at component level are developed, one for a component itself and the other for the connection between two components linked by a joint. On this basis, a number of elementary command templates can be packaged into a compound one for a subassembly, e.g. the revolute joint as shown in Fig.7.

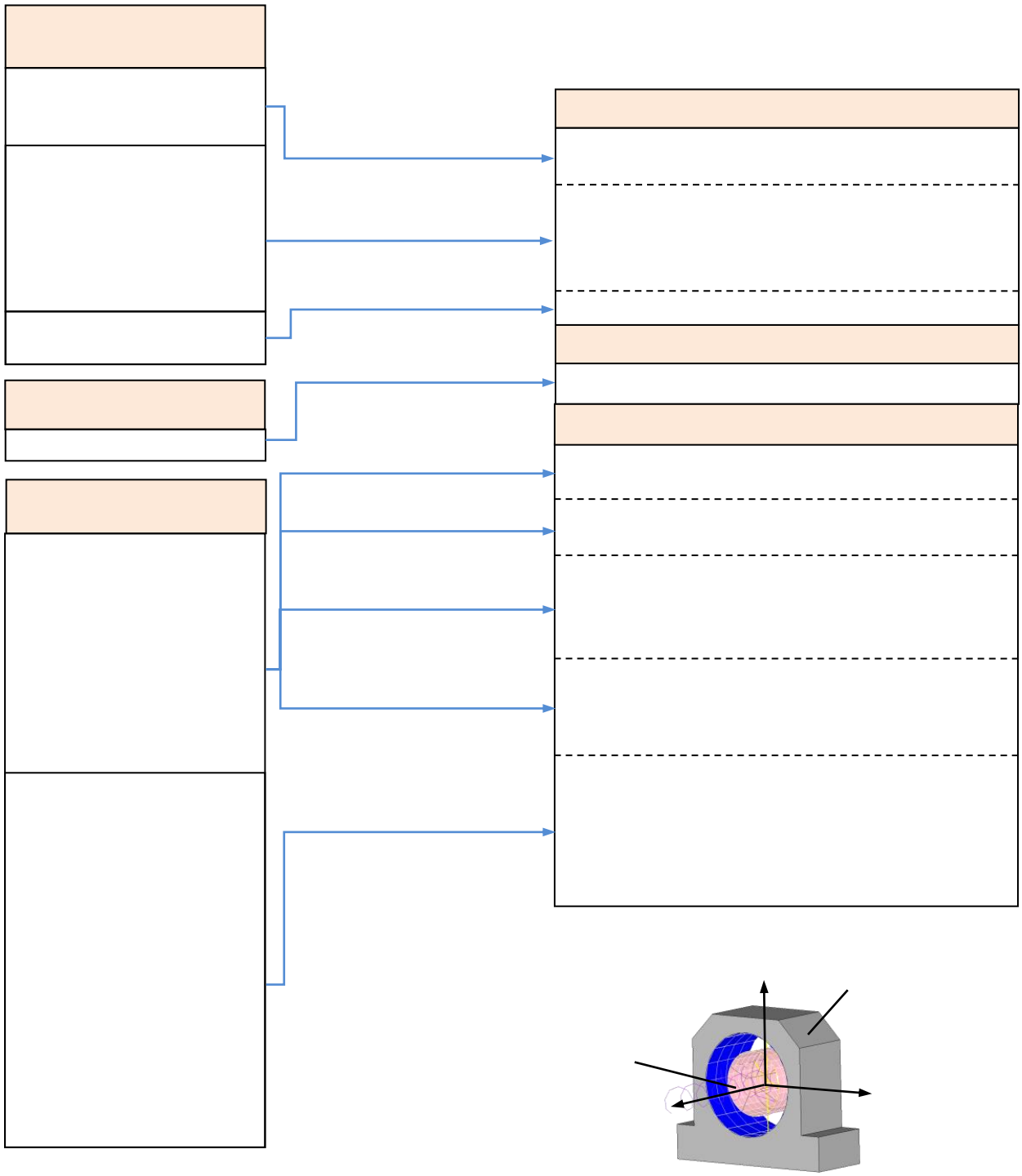

Fig.7. The Bacon command template for a revolute joint

In this way, the FE model of a PKM at a given configuration can be built or modified using the process shown in Fig.8.

(1) Extract the attributes of analysis features at component level (which have been already defined and can be modified in SolidWorks) using SolidWorks API and save them into a file;

(2) Load the attributes of analysis features of components/connections/subassemblies sequentially to the Notebook in a batch mode;

(3) For a specific component/connection/subassembly, load the prescribed command template from the library and assign the

attributes of analysis features to the keywords in form of the Bacon commands;

(4) Implement steps (2) and (3) until the keywords of all components/connections/subassemblies are assigned;

(5) Load the Bacon commands of all components/connections/subassemblies to the Epilogue module situated in SAMCEF solver to create or modify the Bacon script for FE modeling.

Table 1 The keywords of Bacon commands

Keywords	Descriptions	Keywords	Descriptions
MAT	Material properties	**SEL**	Select the related geometric entities
HYP	Element type	**MCE**	Select the assemble element
CLM	Payload imposed upon the selected geometric entities	**MCC**	Assign properties of the assemble element
NOE	Node coordinates	**AEL**	Assign material properties to components

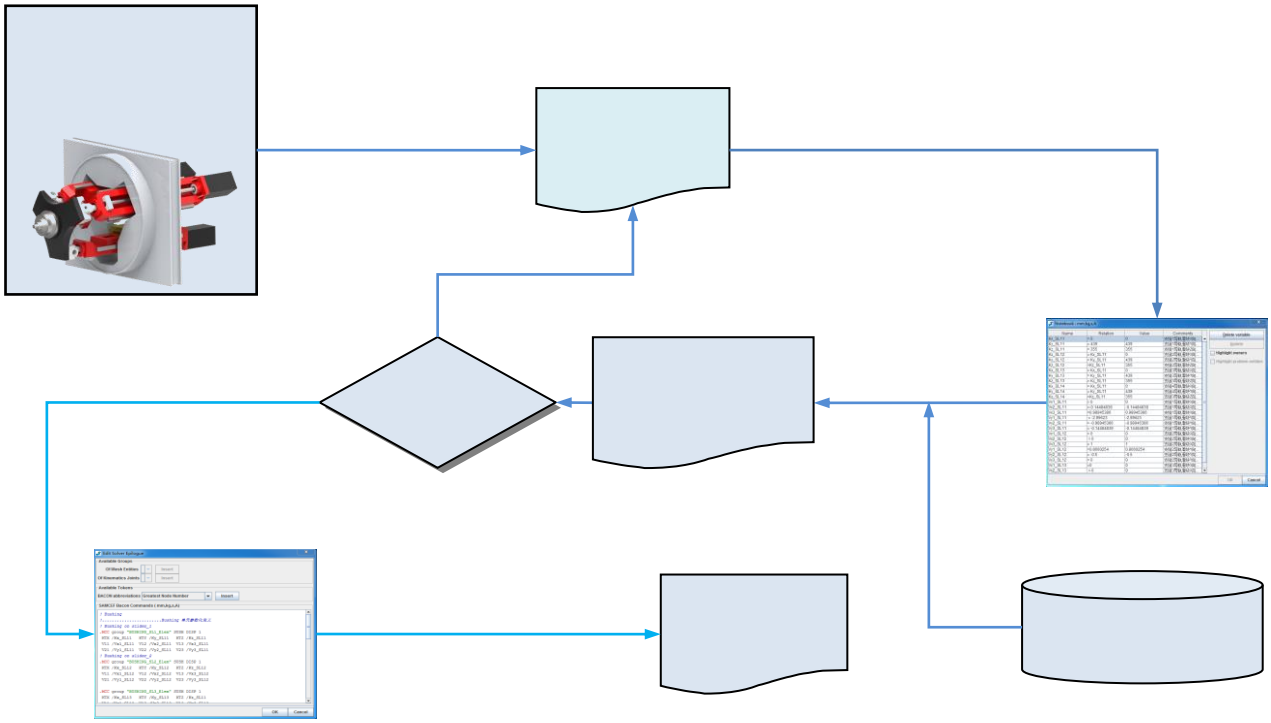

Fig.8. Process to generate Bacon scripts for FE modeling

4. An Example

Following the flow chart shown in Fig.4 and the detailed procedures shown in Figs.5-8, the stiffness analysis and modal analysis are carried out in this section to evaluate the static and dynamic characteristics of the A3 head using the proposed feature-based CAD-CAE integration approach. Also, the validity of the proposed modeling and analysis strategy is verified by experiments.

Fig.9 shows the kinematic diagram of the A3 head with the dimensions given in Table 2, where a and b denote the radii of circumcircles of equilateral triangles $\Delta A_1A_2A_3$ and $\Delta B_1B_2B_3$, c denotes the normal distance of tool tip centre (TCP) P to $\Delta A_1A_2A_3$, and d denotes the distance between $\Delta A_1A_2A_3$ and $\Delta B_1B_2B_3$ when the mechanism situates at the home position. The movement capability of the moving platform can be described by the precession angle of $\psi = 0° \sim 360°$, the nutation angle of $\theta = 0° \sim 40°$, and the stroke of $s = 0 \sim 200$ mm along the z axis [29]. Fig.10 shows the dynamic model of a RPS limb with the corresponding stiffness coefficients given in Tables 3-5. The simulation results shown below are obtained by the FE model built in SAMCEF.

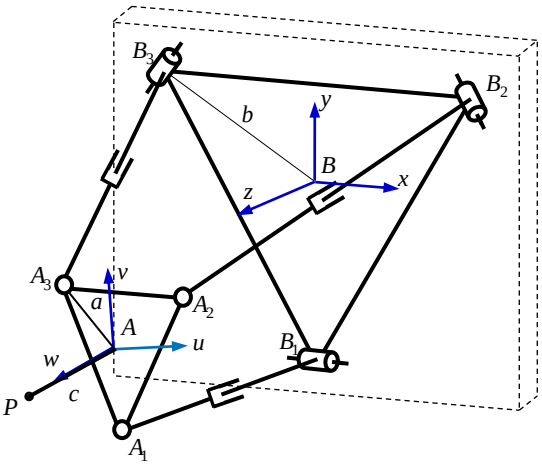

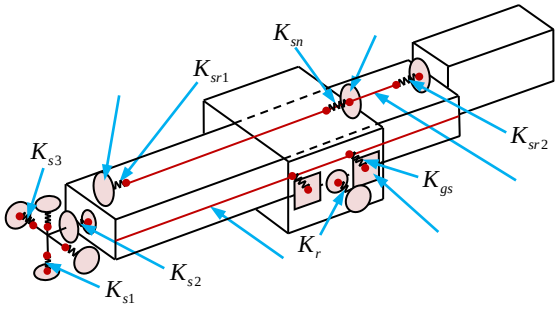

Table 3 Stiffness coefficients of the roll bearings

Location	Axial stiffness K_x (N / μm)	Radial stiffness K_y, K_z (N / μm)	Tilt stiffness K_b, K_c (KN. m / rad)	Rotational stiffness K_a (KN. m / rad)
Short axis of S-joint (K_{s1})	120	86	90	0
Long axis of S-joint (K_{s2})	450	320	245	0
Cross axis of S-joint (K_{s3})	180	120	46	0
R-joint (K_r)	1006	530	146	0
Front-end bearing (K_{sr1})	102	210	69	0
Rear-end bearing (K_{sr2})	1780	1037	556	0

Table 4 Stiffness coefficients of the guideway-slider assembly

Type	Tangential stiffness K_{gsx} (N / μm)	Lateral stiffness K_{gsy} (N / μm)	Normal stiffness K_{gsz} (N / μm)	Roll stiffness K_{gsa} (KN. m / rad)	Pitch stiffness K_{gsb} (KN. m / rad)	Yaw stiffness K_{gsc} (KN. m / rad)
Values	0	789	857	100	330	300

Table 5 Stiffness coefficients of the lead screw-nut assembly

Type	Drive stiffness K_{snx} (N/ μm)	Radial stiffness K_{sny} (N/ μm)	Radial stiffness K_{snz} (N/ μm)	Torsional stiffness K_{sna} (KN. m / rad)	Tilt stiffness K_{snb} (KN. m / rad)	Tilt stiffness K_{snc} (KN. m / rad)
Values	380	1000	1000	19.4	300	300

4.1. Prediction and verification of stiffness

From high-speed milling point of view, it is suitable to evaluate the stiffness of the A3 head in the body-fixed frame $P-uvw$ attached to the platform as shown in Fig.11. Here, F_u, F_v and F_w denote the applied forces imposed at the TCP along the *u*, *v* and *w* axes, and M_w denotes the applied torque about the *w* axis. Based upon the proposed CAD-CAE integration method, the distributions of linear stiffness along the *u*, *v* and *w* axes and the torsional stiffness about the *w* axis over the orientation workspace of $\psi = 0° \sim 360°$, and $\theta = 0° \sim 40°$ can be predicted in a very quick manner. It can be seen from Fig.12 that stiffness along/about three orthogonal axes are tri-symmetrical in nature. K_{tu} and K_{tw} take the maximum value at $\theta = 0°$ and decrease monotonically to the minimum

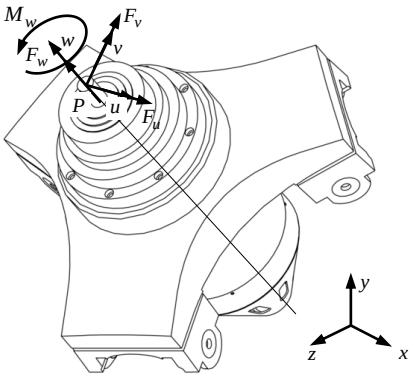

value at $\theta = 40^\circ$, On the contrary, K_{tv} and K_{rw} take the minimum values at $\theta = 0^\circ$ and increase monotonically to the maximum value at $\theta = 40^\circ$. Meanwhile, the distribution of K_{tw} varies little at $s = 200$ mm compared with that at $s = 0$ mm, and the distributions of K_{tu}, K_{tv} and K_{rw} at $s = 200$ mm are relatively smaller than those at $s = 0$ mm due to the decreases of the bending and torsional stiffness of the RPS limbs.

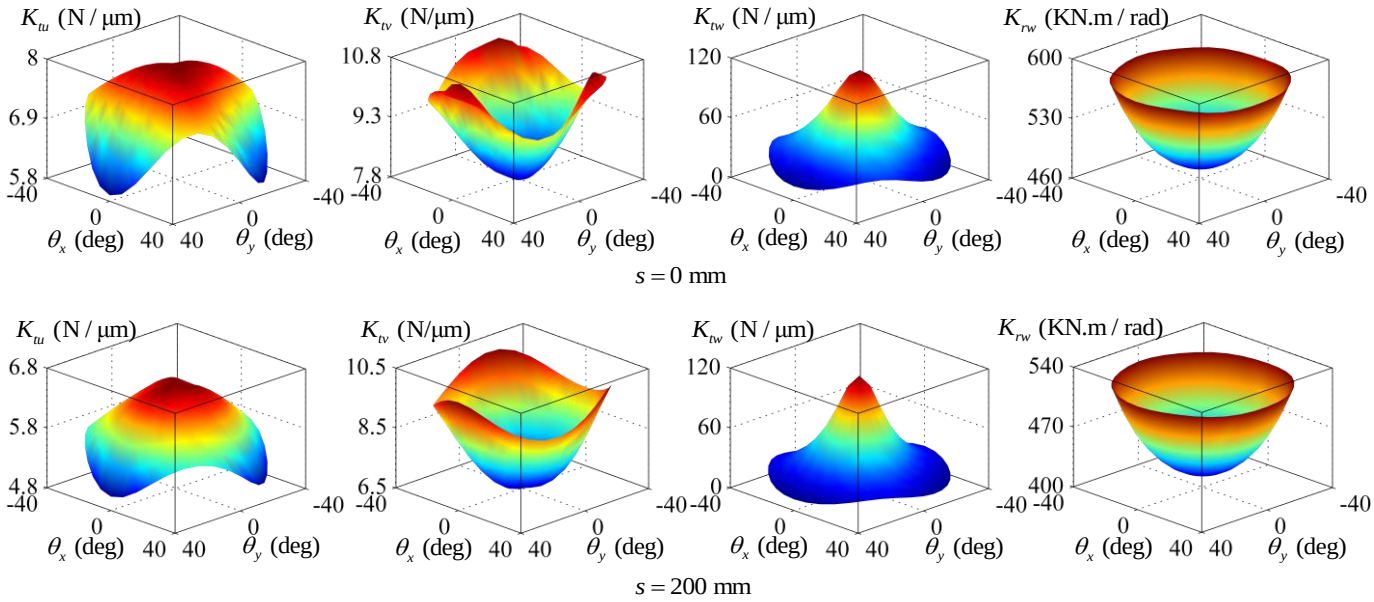

Fig.12. Stiffness distributions over $\psi = 0 \sim 360^\circ, \theta = 0 \sim 40^\circ \left(\theta_x = \theta \sin\psi, \theta_y = \theta \cos\psi\right)$

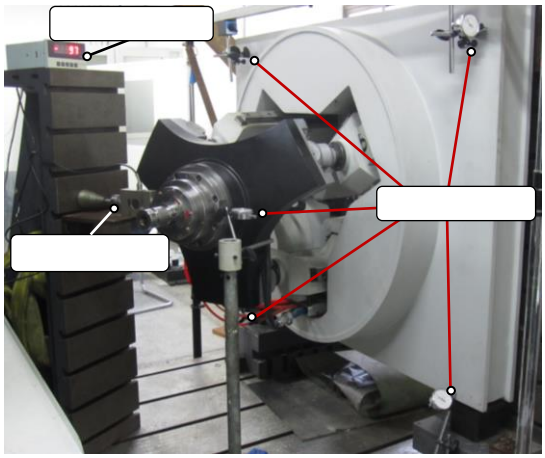

Fig.13. The setup for stiffness test

Table 6 The stiffness at $\psi = 0^\circ$, $\theta = 0^\circ$

K_{tu} / s	0 mm	50 mm	100 mm	150 mm	200 mm
Predicted (N / μm **)**	7.91	7.52	7.15	6.83	6.55
Measured (N / μm **)**	7.88	7.63	7.06	6.59	6.38
Error (%)	0.38	1.44	1.27	3.64	2.66
K_{tv} / s	0 mm	50 mm	100 mm	150 mm	200 mm
Predicted (N / μm **)**	7.82	7.47	7.08	6.75	6.50
Measured (N / μm **)**	8.22	7.88	7.10	6.43	6.18
Error (%)	4.87	5.20	0.28	4.98	5.18

Stiffness test was carried out on the prototype of the A3 head to verify the results of computer simulations. In the experiment, the force along a given direction was applied at the TCP by a screw jack and measured by a force gauge, and the deformations of

the platform and the base were measured by dial indicators as shown in Fig.13. Given $\psi = 0^\circ$ and $\theta = 0^\circ$, Tables 6 shows the stiffness at TCP along the *u* and v axes when stroke *s* increases with an increment of 50 mm from 0 mm to 200 mm. It can be seen that the maximum discrepancy of the predicted values away from the measured ones is less than 6%. The discrepancies may be attributed to the differences between the joint stiffness specified by product catalogues [36-38] and that in the real prototype. The reasons for these differences may be the idealization of joints with linear springs in the simulation, as well as the manufacturing and assembling errors which can affect the joint behavior of the physical prototype.

4.2. Prediction and verification of dynamic behaviours

The dynamic behaviors of the A3 head over the entire workspace can also be rapidly predicted using the proposed CAD-CAE integration system. Fig.14 shows the distributions of the first three natural frequencies at $s = 0$ mm and $s = 200$ mm, respectively. It can be seen that in the case of $s = 0$ mm, f_1 takes the maximum value at $\theta = 0^\circ$ and the minimum value at $\theta = 40^\circ$. On the contrary, f_2 and f_3 take the minimum value at $\theta = 0^\circ$ and the maximum values at $\theta = 40^\circ$. In the case of $s = 200$ mm, the distribution of f_1 is similar to that when $s = 0$ mm, but the distributions of f_2 and f_3 are quite different to those at $s = 0$ mm because of changes in mode shapes. Also, it is interesting to see that the first three natural frequencies increase along with the increase of stroke s from 0 mm to 200 mm though the stiffness decreases with the increase of the stroke, indicating that the mass center location of the limb relative to the R joint has significant bearings on the natural frequencies of the system.

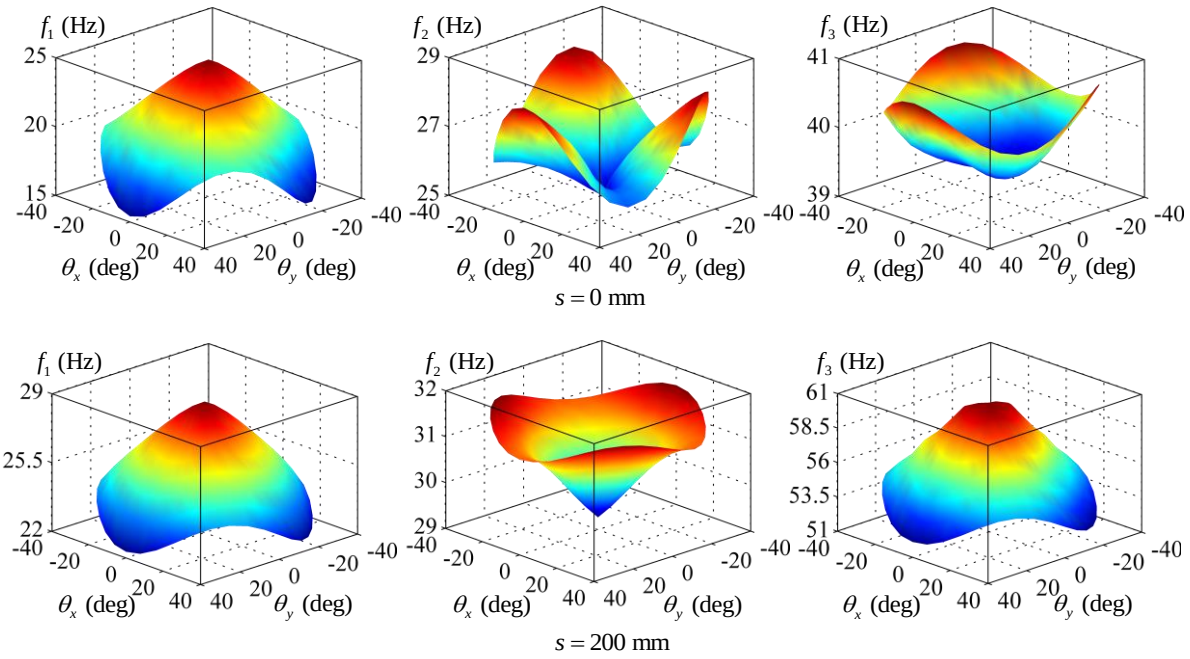

Fig.14. Natural frequency distributions over $\psi = 0 \sim 360^\circ, \theta = 0 \sim 40^\circ \left(\theta_x = \theta \sin\psi,\ \theta_y = \theta \cos\psi\right)$

The experimental modal analysis was also carried out to verify the predicted dynamic behaviors of the prototype using impact excitation method with the setup shown Fig.15, allowing the comparison to be made between the measured and predicted Frequency Response Functions (FRFs) at $\psi = 0^\circ$, $\theta = 0^\circ$ and $s = 200$ mm as shown in Fig.16. It can be seen from Fig.16 and Table 7 that the predicted FRFs with the assumed damping ratio of $\eta = 0.02$ have good match to those obtained by the experimental modal analysis, thus proving the accuracy of the proposed approach. On this basis, the distributions of FRFs varying with the system configurations were predicted and measured. Fig.17 shows the amplitude vs. frequency curves when stroke *s* varies from 0 mm to 200 mm with $\theta = 0^\circ$, and when nutation angle θ varies from -30° to 30° with $s = 200$ mm and $\psi = 0^\circ$, respectively. It is observed again that the predicated FRFs have good match to the measured ones at different configurations, thus laying a solid ground for cutting stability prediction.

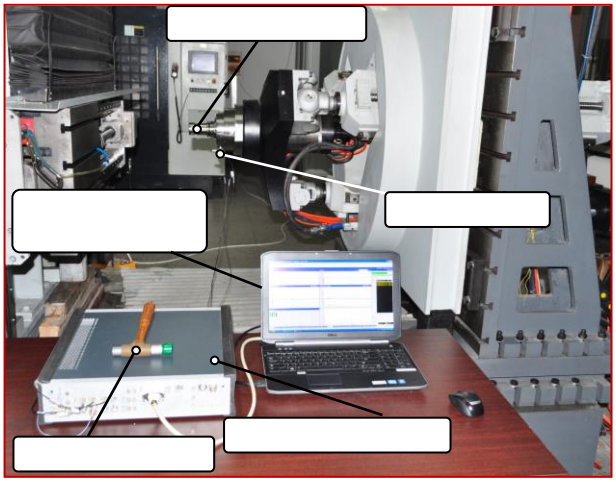

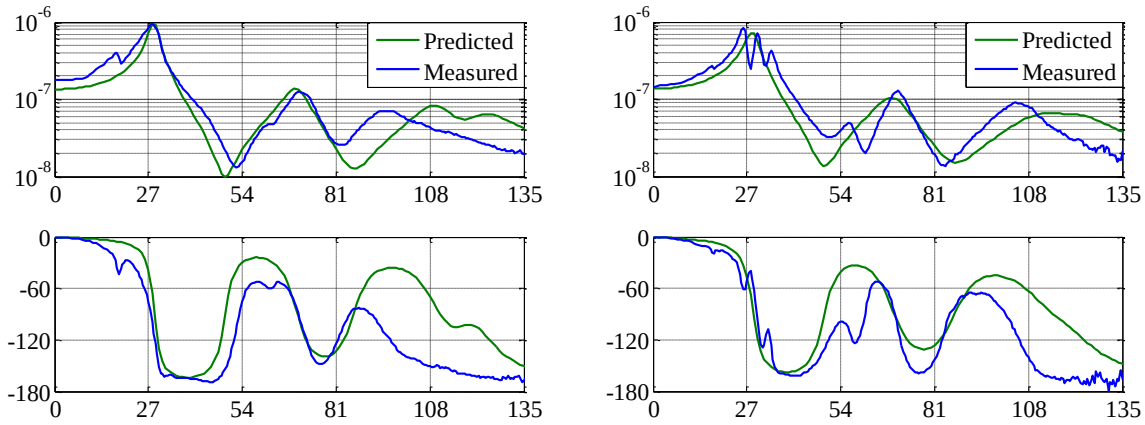

Fig.16. The measured and predicted TCP FRFs at ψ=0°, θ=0° and $s = 200$ mm

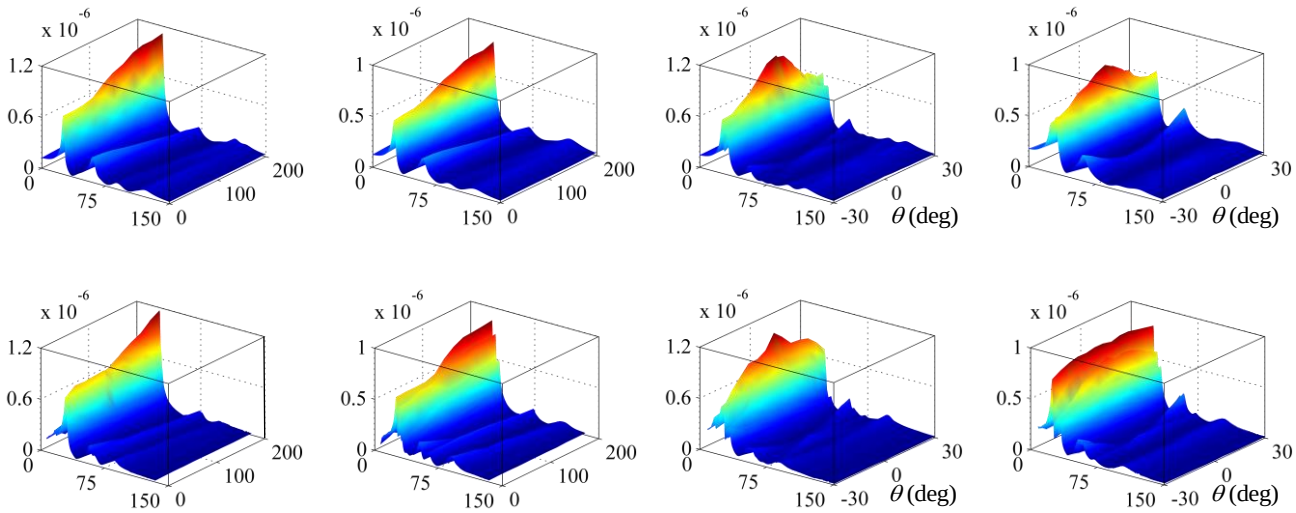

Fig.17. The predicted and measured FRFs varying with the system configurations

5. Conclusions

This paper presents a CAD-CAE integration approach for static and dynamic performance evaluation of a PKM spindle head

over its entire workspace. The following conclusions are drawn:

(1) By automatically mapping the configuration and analysis features from the CAD system (SolidWorks) to the CAE system (SAMCEF), the framework and detailed procedures for the feature-based CAD-CAE integration are proposed to allow the static and dynamic performances over the task workspace of the A3 head to be evaluated in a very quick manner.

(2) By exploiting the assembly elements provided by CAE, a method for FE modeling of the commonly used joints and subassemblies in PKMs is proposed to significantly improve the computational accuracy and efficiency.

(3) The accuracy of the proposed approach is verified by showing that the predicted values in terms of rigidity, natural frequency and FRFs have good match to those obtained by experiments at various configurations.

(4) The proposed approach is general and it thereby can be employed for the design and performance prediction of the PKMs having a wide variety of topological architectures.

(5) Further work will be carried out to enrich the frequently used object-oriented models of analysis features and illustrate the effectiveness of the proposed approach in static and dynamic performance optimization. These issues, however, deserve to be addressed in separate articles.

Acknowledgements

This work is partially supported by the National Natural Science Foundation of China (NSFC) under grant 51135008.

References

[1] Weck M, Staimer D. Parallel kinematic machine tools-current state and future potentials. CIRP Annals-Manufacturing Technology 2002; 51(2): 617-683.

[2] Xie F, Liu XJ, Wang J. A 3-DOF parallel manufacturing module and its kinematic optimization. Robotics and Computer-Integrated Manufacturing 2012; 28(3): 334-343.

[3] Altintas Y, Brecher C, Weck M, Witt S. Virtual machine tools. CIRP Annals-Manufacturing Technology 2005; 54(2): 115-138.

[4] Bianch G, Tosatti LM, Fassi I. Virtual prototyping of parallel mechanisms. ImechE Proc Instn Mech Engrs Part K: Journal of Multi-body Dynamics 2002; 216(1): 21-37.

[5] Zhang D, Wang L, Lang SY. Parallel kinematic machines: design, analysis and simulation in an integrated virtual environment. Journal of Mechanical Design 2005; 127(4): 580-588.

[6] Wang YY, Huang T, Zhao XM, Mei JP, Chetwynd DG, Hu SJ. Finite element analysis and comparison of two hybrid robots-the Tricept and the TriVariant. Intelligent Robots and Systems, 2006 IEEE/RSJ International Conference on. IEEE, 2006: 490-495.

[7] Xu B, Chen N. An integrated method of CAD, CAE and multi-objective optimization. Computer-Aided Industrial Design & Conceptual Design, 2009. CAID & CD 2009. IEEE 10th International Conference on. IEEE, 2009:1010-1014.

[8] Chung TT, Lee CC, Fan KC. Optimal design of a 1×2 mechanical optical switch. Structural and Multidisciplinary Optimization 2006; 31(3): 229-240.

[9] Park HS, Dang XP. Structural optimization based on CAD-CAE integration and metamodeling techniques. Computer-Aided Design 2010; 42(10): 889-902.

[10] Kao YC, Cheng HY, She CH. Development of an integrated CAD/CAE/CAM system on taper-tipped thread-rolling die-plates. Journal of Materials Processing Technology 2006; 177(1): 98-103.

[11] Dang XP. General frameworks for optimization of plastic injection molding process parameters. Simulation Modeling Practice and Theory 2014; 41: 15-27.

[12] Wang D, Hu F, Ma Z, et al. A CAD/CAE integrated framework for structural design optimization using sequential approximation optimization. Advances in Engineering Software 2014; 76: 56-68.

[13] Yin CG, Ma YS. Parametric feature constraint modeling and mapping in product development. Advanced Engineering Informatics 2012; 26(3): 539-552.

[14] Li WD, Ong SK, Fuh JYH, et al. Feature-based design in a distributed and collaborative environment. Computer-Aided Design 2004; 36(9): 775-797.

[15] Chen G, Ma YS, Thimm G, et al. Unified feature modeling scheme for the integration of CAD and CAx. Computer Aided Design & Applications 2004; 1(1-4): 595-602.

[16] Aifaoui N, Deneux D, Benamara A, et al. Mechanical analysis process modeling based on analysis features. Systems, Man and Cybernetics, 2002 IEEE International Conference On. IEEE, 2002; 3: 636-640.

[17] Gao S, Zhao W, Lin H, Yang F, Chen X. Feature suppression based CAD mesh model simplification. Computer-Aided Design 2010; 42(12): 1178-1188.

[18] Li B, Liu J. Detail feature recognition and decomposition in solid model. Computer-Aided Design 2002; 34(5): 405–414.

[19] Arabshahi S, Barton D C, Shaw NK. Steps towards CAD-FEA integration. Engineering with Computers 1993; 9(1): 17-26.

[20] Deng YM, Britton GA, Lam YC, Tor SB, Ma YS. Feature-based CAD-CAE integration model for injection-moulded product design. International Journal of Production Research 2002; 40(15): 3737-3750.

[21] Niu WT, Wang PF, Shen Y, et al. A feature-based CAD-CAE integrated approach of machine tool and its implementation. Advanced Materials Research 2011; 201: 54-58.

[22] Lee SH. A CAD-CAE integration approach using feature-based multi-resolution and multi-abstraction modeling techniques.

Computer-Aided Design 2005; 37(9): 941-955.
[23] Gujarathi GP, Ma YS. Parametric CAD/CAE integration using a common data model. Journal of Manufacturing System 2011; 30(3): 118-132.
[24] Hamri O, Léon JC, Giannini F, et al. Software environment for CAD/CAE integration. Advances in Engineering Software 2010; 41(10): 1211-1222.
[25] Xia Z, Wang Q, Wang Y, et al. A CAD/CAE incorporate software framework using a unified representation architecture. Advances in Engineering Software 2015; 87: 68-85.
[26] Kong X, Chang SI, Yin L, et al. Rapid integrated parametric CAE modeling method of Linear Variable Differential Transformer based on a script template. Advances in Engineering Software 2015; 86: 13-19.
[27] Liu J, Ma Y, Fu J, et al. A novel CACD/CAD/CAE integrated design framework for fiber-reinforced plastic parts. Advances in Engineering Software 2015; 87: 13-29.
[28] Huang T, Liu HT. A Parallel Manipulator with Two Orientations and One Translation. Patent No. WO/PCT/2007/124637; 2007.
[29] Li YG, Liu HT, Zhao XM, Huang T, Chetwynd DG. Design of a 3-DOF PKM module for large structural component machining. Mechanism and Machine Theory 2010; 45(6): 941-954.
[30] Neumanm KE. Robot. US.Patent No.4732525; 1988-3-22.
[31] Neumanm KE. Parallel-kinematical machine. Patent No. WO/2006/054935; 2006.
[32] Hennes N, Staimer D. Application of PKM in aerospace manufacturing-high performance machining centers ECOSPEED, ECOSPEED-F and ECOLINER. Proceedings of the 4th Chemnitz Parallel Kinematics Seminar, 2004: 557-568.
[33] Maj R, Bianchi G. Mechatronic analysis of machine tools. 9th SAMTECH Users Conference, 2005.
[34] Bruyneel M, Granville D. Mechatronic analysis of a flexible mechanism using SAMCEF: application to robotics. Proceedings of the NAFEMS Copenhagen, 2007.
[35] SolidWorks premium package-2010 (SolidWorks+CosmosMotion+CosmosWorks). SolidWorks Corporation. <http:// www.solidworks.com>, 2014.
[36] LuoYang Bearing. (<http://www.lyc.cn>).
[37] INA Co. Ltd. Deutschland. (<http://www.ina.de/content.ina.de/de/index.jsp >).
[38] THK Co. Ltd. (<http://www.thk.com>).

Listing of figure captions:

Fig.1. CAD model of the A3 head

Fig.2. FE modeling of a 1-DOF joint using assembly elements

Fig.3. Joint FE models in the A3 head

Fig.4. The flow chart of the proposed CAD-CAE integration

Fig.5. The object-oriented model of analysis features

Fig.6. The process to update the configuration of the CAD model in SAMCEF

Fig.7. The Bacon command template for a revolute joint

Fig.8. Process to generate Bacon scripts for FE modeling

Fig.9. A schematic diagram of the A3 head

Fig.10. Dynamic model of a RPS limb

Fig.11. Cutting forces and torque applied at the tool tip center

Fig.12. Stiffness distributions over $\psi = 0 \sim 360^\circ, \theta = 0 \sim 40^\circ \left(\theta_x = \theta \sin\psi,\ \theta_y = \theta \cos\psi\right)$

Fig.13. The setup for stiffness test

Fig.14. Natural frequency distributions over $\psi = 0 \sim 360^\circ, \theta = 0 \sim 40^\circ \left(\theta_x = \theta \sin\psi,\ \theta_y = \theta \cos\psi\right)$

Fig.15. The setup for FRF measurement

Fig.16. The measured and predicted TCP FRFs at $\psi = 0^\circ$, $\theta = 0^\circ$ and $s = 200$ mm

Fig.17. The predicted and measured FRFs varying with the system configurations